Proceedings of the 17th Danube European Conference on Geotechnical Engineering (17DECGE)
June 7-9, 2023, Bucharest, România

"*p-y*" curves for piles in radially inhomogeneous soil

A.H. Bateman[1], G. Mylonakis[1,2]

[1] Department of Civil Engineering, University of Bristol, UK
[2] Department of Civil, Infrastructure and Environmental Engineering, Khalifa University, Abu Dhabi, UAE

Abstract. "*p-y*" curves are used to simplify the pile response of laterally loaded piles at any given depth by describing the applied lateral soil reaction as a function of the lateral displacement. Simple analytical solutions in two-dimensions for system stiffness are available by modelling a segment of the pile surrounded by an annular zone of linear-elastic soil. Current solutions assume homogeneous soil conditions. However, installation of a bored pile in clay would result in a region of softened material immediately surrounding the pile-soil interface, which can be modelled using a function describing the variation of shear modulus with distance from the pile. Such functions are available in the literature using linear and power-law variations. This paper derives an improved solution for the system stiffness considering the effects of pile installation. The previously discussed annular zone of soil is split into multiple rings with each able to define an independent shear modulus. A solution for the overall system stiffness is provided. Three-dimensional and parameter effects are discussed.

Keywords: Laterally loaded piles; "p-y" curves; Radial inhomogeneity

1 INTRODUCTION

Analysis of laterally loaded piles can be simplified by discretising the pile-soil system into multiple horizontal soil "slices" of infinitesimal thickness. For each slice at a specific depth, the behaviour can be modelled using (1) a "*p-y*" curve describing the lateral displacement resulting from a corresponding load; (2) and an "*m-θ*" curve describing the pile rotation under a corresponding moment (e.g. Byrne *et al.* 2020; Bateman *et al.* 2023; beyond the scope of this work). A numerical integration approach can then be applied to compute the overall lateral deflection under a given load.

A simplified method to determine a "*p-y*" curve simplifies the three-dimensional continuum problem using a horizontal slice through the pile. The pile slice is surrounded by a soft "inner" annular zone of homogenous soil of finite radius, which is surrounded by a semi-infinite "outer" annular zone of homogeneous soil of infinite radius with a higher modulus than in the inner zone (Novak and Sheta 1980). The overall system stiffness is calculated by combining the compliance of the "inner" and "outer" rings by modelling them as a pair of springs in series. Evidently, this approach is approximate because compatibility of displacements at the interface between the rings is not rigorously considered (discussed later in this paper). The behaviour of the "inner" zone has been considered in the literature and closed-form solutions are available for various response modes under static and dynamic loading. These include: horizontal (e.g. Karatzia *et al.* 2014), vertical (e.g. Michaelides *et al.* 1998; El Naggar 2000), rotation or rocking (e.g. Novak *et al.* 1978; Lakshmanan and Minai 1981) and torsional (e.g. El Naggar 2000) modes. Similarly, the behaviour of the "outer" zone has been considered (e.g. Baguelin *et al.* 1977; Novak *et al.* 1978; Mylonakis 2001; Karatzia and Mylonakis 2017; Crispin and Mylonakis 2022).

The above solutions assume radially homogeneous soil. However, installation of the pile will result in a "disturbed" region immediately surrounding the pile circumference. Specifically, O'Neill (2001)

suggested that bored pile installation results in larger reductions of soil stiffness closer to the pile-circumference. This was verified experimentally by Kalinski and Stokoe (1998) and Kalinski *et al.* (2001) who used Spectral Analysis of Surface Waves (SASW) techniques to measure the radial variation of shear modulus in the vicinity of a bored pile. This variation of shear modulus with radial distance has been modelled using a linear variation by Kraft *et al.* (1981) and using a power-law variation by Bateman and Crispin (2020). Following on from this, the horizontal slice approach discussed above, has also been used for radially inhomogeneous soil for vertical, rocking, and torsional modes (e.g. Lakshmanan and Minai 1981; Veletsos and Dotson 1988; Han and Sabin 1995). It has also been employed for dynamic horizontal loading by Lakshmanan and Minai (1981) and Veletsos and Dotson (1988). However, there is a lack of solutions for lateral loading under static conditions which provides the motivation for this work.

This paper develops an extension to the available solutions for the stiffness of the "inner" annular zone under homogeneous conditions to consider the effects of pile installation. To achieve this, the "inner" annular zone is split into multiple rings with each able to define an independent shear modulus. The addition of the "outer" annular zone to compute an overall system stiffness (that includes three-dimensional effects) is discussed.

2 PROBLEM DEFINITION

A circular horizontal slice of soil of infinitesimal thickness is considered (Fig. 1). A rigid pile segment of radius r_0, is surrounded by an annular zone of homogeneous, linear-elastic soil of shear modulus G and Poisson's ratio ν. Extension of the analysis to include a radial variation of shear modulus is discussed later in this paper. Cylindrical coordinates are defined using r as the distance from the centre of the pile and θ as the aperture angle. A fictitious rigid boundary is assumed at a distance $r = b$, the effect of which is discussed later in this paper. Perfectly rough interfaces are considered at the pile-soil interface ($r = r_0$) and at the outer boundary ($r = b$), as was assumed by Novak and Sheta (1980). Alternative assumptions for interface roughness are explored in Karatzia *et al.* (2014).

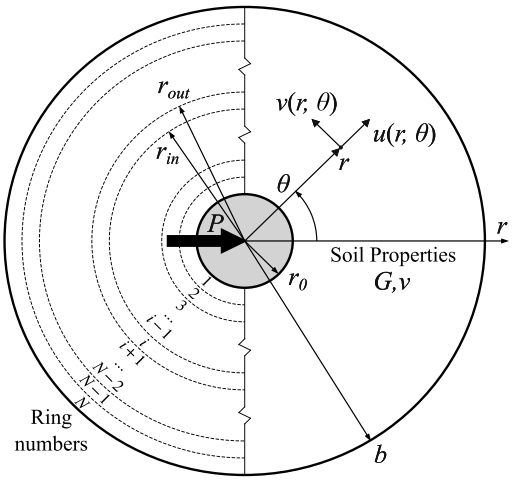

Figure 1. Plan view of the "inner" ring of a horizontal soil slice showing the problem geometry and the proposed discretisation.

A constant lateral load P is applied to the pile, acting at $\theta = 0$. This leads to a lateral movement of the pile which results in a deformation mechanism within the annular soil zone which can be defined using radial $u(r, \theta)$ and tangential $v(r, \theta)$ displacements. In the realm of this model, the radial, u, and tangential, v, displacement components can be given by (Novak and Sheta 1980, Karatzia *et al.* 2014):

$$u(r,\theta) = \frac{1}{2G}\left[A_1\left[(3-4\nu)\ln\left(\frac{r}{r_0}\right)-1\right] + A_2(3-4\nu) + A_3(1-4\nu)\left(\frac{r}{r_0}\right)^2 + A_4(5-4\nu)\left(\frac{r}{r_0}\right)^{-2}\right]\cos\theta \qquad (1a)$$

$$v(r,\theta) = \frac{1}{2G}\left[-A_1(3-4\nu)\ln\left(\frac{r}{r_0}\right) - A_2(3-4\nu) + A_3(5-4\nu)\left(\frac{r}{r_0}\right)^2 + A_4(5-4\nu)\left(\frac{r}{r_0}\right)^{-2}\right]\sin\theta \quad (1b)$$

where A_1, A_2, A_3 and A_4 are integration constants. The strains, ε_{rr}, $\varepsilon_{\theta\theta}$ and $\varepsilon_{r\theta}$, within the medium can be calculated using standard field relations in polar coordinates [$\varepsilon_{rr} = \partial u/\partial r$, $\varepsilon_{\theta\theta} = (\partial v/\partial\theta + u)/r$ and $\varepsilon_{r\theta} = 1/2\,[\partial v/\partial r - v/r + (\partial u/\partial\theta)/r]$] to get:

$$\begin{bmatrix}\varepsilon_{rr}/\cos\theta \\ \varepsilon_{r\theta}/\sin\theta \\ \varepsilon_{\theta\theta}/\cos\theta\end{bmatrix} = \frac{1}{2Gr^3r_0^2}\begin{bmatrix} r^2r_0^2(3-4\nu) & 2r^4(1-4\nu) & -2r_0^4(5-4\nu) \\ -r^2r_0^2(1-2\nu) & 2r^4 & -2r_0^4(5-4\nu) \\ -r^2r_0^2 & 2r^4(3-4\nu) & 2r_0^4(5-4\nu)\end{bmatrix}\begin{bmatrix}A_1 \\ A_3 \\ A_4\end{bmatrix} \quad (2)$$

Perfect bonding is assumed at the pile-soil interface [$u(r_0,0) = u_0$ and $v(r_0,\pi/2) = -u_0$] and at the outer surface [$u(b,\theta) = 0$ and $v(b,\theta) = 0$] (Novak and Sheta 1980). Applying these constraints to Eq. 1 enables A_1, A_2, A_3 and A_4 to be determined analytically and are given explicitly in Karatzia *et al.* (2014). By considering a unit pile displacement, the sum of the tangential and radial tractions at the pile circumference yields the stiffness of the system k (Karatzia *et al.* 2014).

$$k = -r_0\int_0^{2\pi}[\sigma_{rr}(r_0,\theta)\cos\theta - \tau_{r\theta}(r_0,\theta)\sin\theta]\,d\theta = -\pi\, r_0\left[\sigma_{rr}(r_0,0) - \tau_{r\theta}\left(r_0,\frac{\pi}{2}\right)\right] \quad (3)$$

where σ_{rr} and $\tau_{r\theta}$ are normal and shear stresses, respectively. Assuming a linear-elastic soil of shear modulus G and Poisson's ratio ν, the corresponding stress to the strain in Eq. 2 can be obtained using Hooke's law. Substituting these into Eq. 3 yields the closed-form expression (Novak and Sheta 1980):

$$k = G\frac{8\pi(3-4\nu)(1-\nu)\left[(b/r_0)^2+1\right]}{1-(b/r_0)^2+(3-4\nu)^2\left[(b/r_0)^2+1\right]\ln\left(\frac{b}{r_0}\right)} \quad (4)$$

Evidently, this solution is dependent on the distance to the outer boundary b, the pile radius r_0, and the soil material constants G, ν. Some basic trends can be noted; the system stiffness k (1) has the same units as the shear modulus G; (2) is proportional to G; (3) decreases monotonically with increasing material thickness b/r_0 (from infinity for a very thin annular zone, to zero for an unbounded medium); (4) increases monotonically with increasing Poisson's ratio to a maximum value for an incompressible medium. Asymptotic relations for thin and thick annular zones are discussed in Karatzia *et al.* (2014).

3 RADIAL INHOMOGENEITY

Eq. 4 assumes a homogeneous, linear-elastic soil medium of constant shear modulus, G. However, G is often a function of r as pile installation results in a softened zone close to the pile circumference, resulting in radially varying soil properties (Fig. 2). Following Veletsos and Dotson (1988), radial inhomogeneity can be applied to the solution above by splitting the inner zone into N rings (Fig. 1). An independent shear modulus can be selected for each ring, G_i, which can be calculated at the centre of the ring from a continuous function $G(r)$. Employing this technique, the displacements (Eq. 1) and stresses (from Eq. 2) can be written in matrix form for a general ring i, with shear modulus G_i

$$\begin{Bmatrix}u(r)/\cos\theta \\ v(r)/\sin\theta \\ \sigma(r)/\cos\theta \\ \tau(r)/\sin\theta\end{Bmatrix}_i = \begin{bmatrix} \frac{\left[(3-4\nu)\ln\left(\frac{r}{r_0}\right)-1\right]}{2G_i} & \frac{(3-4\nu)}{2G_i} & \frac{(1-4\nu)\left(\frac{r}{r_0}\right)^2}{2G_i} & \frac{(5-4\nu)\left(\frac{r}{r_0}\right)^{-2}}{2G_i} \\ -\frac{(3-4\nu)\ln\left(\frac{r}{r_0}\right)}{2G_i} & -\frac{(3-4\nu)}{2G_i} & \frac{(5-4\nu)\left(\frac{r}{r_0}\right)^2}{2G_i} & \frac{(5-4\nu)\left(\frac{r}{r_0}\right)^{-2}}{2G_i} \\ \frac{(3-2\nu)}{r} & 0 & \frac{2r}{r_0^2} & -\frac{2r_0^2(5-4\nu)}{r^3} \\ -\frac{(1-2\nu)}{r} & 0 & \frac{2r}{r_0^2} & -\frac{2r_0^2(5-4\nu)}{r^3}\end{bmatrix}_i \begin{Bmatrix}A_1 \\ A_2 \\ A_3 \\ A_4\end{Bmatrix}_i \quad (5a)$$

which is valid for $[r_{in}]_i \leq r \leq [r_{out}]_i$ (illustrated in Fig. 1). This can be expressed in compact form as:

$$\{\mathbf{S}_v(r)\}_i = [\mathbf{\Delta}(r)]_i\{\mathbf{A}\}_i \tag{5b}$$

where $\mathbf{S}_v$ stands for the state vector in the left-hand side of Eq. 5a and $\mathbf{A}$ is the vector of the unknown integration constants. For general ring i, this equation can be evaluated twice, (1) at the inner boundary ($r = r_{in}$) and (2) the outer boundary ($r = r_{out}$). Solving the first of these equations for $\mathbf{A}$ and substituting into the second yields:

$$\{\mathbf{S}_v(r_{out})\}_i = [\mathbf{\Delta}(r_{out})]_i[\mathbf{\Delta}(r_{in})]_i^{-1}\{\mathbf{S}_v(r_{in})\}_i = [\boldsymbol{\Lambda}]_i\{\mathbf{S}_v(r_{in})\}_i \tag{6}$$

where $[\boldsymbol{\Lambda}]_i = [\mathbf{\Delta}(r_{out})]_i[\mathbf{\Delta}(r_{in})]_i^{-1}$ is the so-called transfer matrix relating the state vector at the two ends of the ring. This equation can be written for each ring by defining r_{in} and r_{out}. Considering equilibrium of forces and continuity of displacements at the interface between rings i and $(i-1)$ it is evident that $\{\mathbf{S}_v(r_{out})\}_{i-1} = \{\mathbf{S}_v(r_{in})\}_i$. Therefore, the state vector for the outermost ring can be written in terms of the state vector of the inner most ring and the product of transfer matrices between each ring:

$$\{\mathbf{S}_v(b)\}_N = \prod_{i=1}^{N}[\boldsymbol{\Lambda}]_i\,\{\mathbf{S}_v(r_0)\}_1 = [\boldsymbol{M}]\{\mathbf{S}_v(r_0)\}_1 \tag{7}$$

To determine the overall stiffness, boundary conditions can be applied to Eq. 7. Considering perfect rigidity at the outer boundary $[u(b) = v(b) = 0]$ and a maximum displacement of u_0 at the pile circumference $[u(r_0) = -v(r_0) = u_0]$, these conditions can be substituted in to give:

$$\begin{Bmatrix} 0 \\ 0 \\ \sigma_{rr}(b)/\cos\theta \\ \tau_{r\theta}(b)/\sin\theta \end{Bmatrix} = \begin{bmatrix} M_{11} & M_{12} & M_{13} & M_{14} \\ M_{21} & M_{22} & M_{23} & M_{24} \\ M_{31} & M_{32} & M_{33} & M_{34} \\ M_{41} & M_{42} & M_{43} & M_{44} \end{bmatrix} \begin{Bmatrix} u_0/\cos\theta \\ -u_0/\sin\theta \\ \sigma_{rr}(r_0)/\cos\theta \\ \tau_{r\theta}(r_0)/\sin\theta \end{Bmatrix} \tag{8}$$

Rearranging this equation for the stresses at the pile circumference and substituting into Eq. 3 (once again setting $u_0 = 1$), yields the system stiffness for radially inhomogeneous soil:

$$k = -r_0 \int_0^{2\pi} \left[\left(\frac{M_{14}M_{21} - M_{24}M_{11}}{M_{13}M_{24} - M_{14}M_{23}} \right) cos\,\theta - \left(\frac{M_{13}M_{22} - M_{23}M_{12}}{M_{13}M_{24} - M_{14}M_{23}} \right) \sin\theta \right] d\theta \tag{9}$$

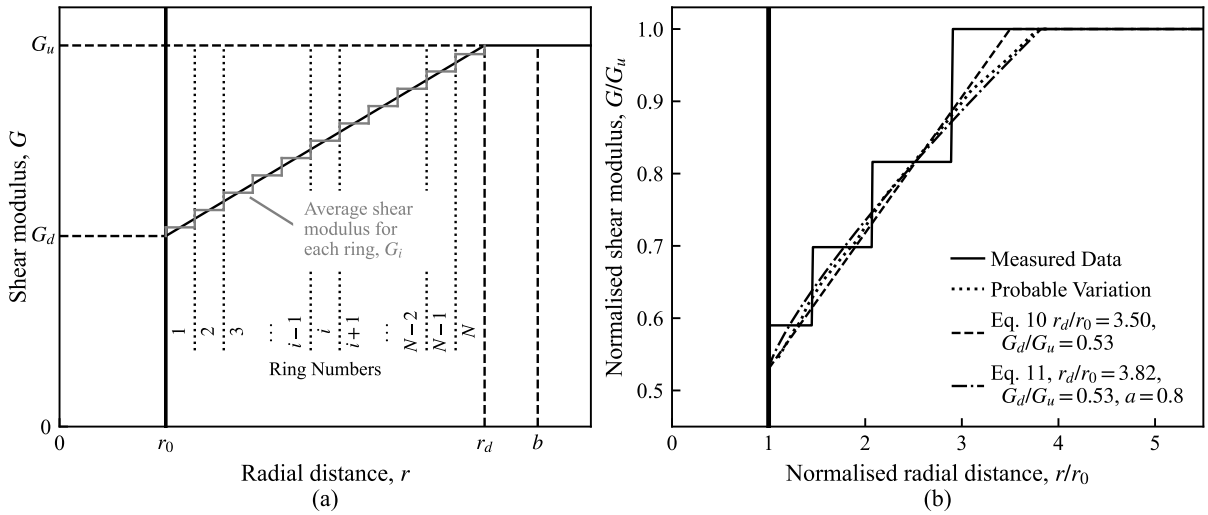

Figure 2. Variation of shear modulus with distance from the pile-soil interface (a) Idealised, (b) fitted functions plotted against O'Neill's "probable variation" (2001). Measured data attributed to Kalinski and Stoke (1998). Fig. 2b reproduced from Bateman and Crispin (2020).

The system stiffness can be calculated using this equation in common spreadsheet software dependent on the number of rings, N, with a separate shear modulus value selected for each ring, G_i. A continuous function $G(r)$ can be defined with a "disturbed" shear modulus G_d (the shear modulus at the pile-soil interface after installation) and an "undisturbed" shear modulus G_u (the constant shear modulus value before pile installation) for $r_0 < r < b$. G_u is reached at the radius of the disturbed material as a result of pile installation r_d. This is shown in Fig. 2a with a linear variation (in black). As r_d is incorporated to model the soft region surrounding the pile, b will often be set as equal to this radius (discussed further below). The radial distance is then split into rings and each ring is assumed to have a constant shear modulus equal to that at the centre of each ring (in grey, Fig. 2a).

Some variations of shear modulus with radial distance as a result of bored pile installation are available in the literature. Kalinski *et al.* (2001) investigated the effects of pile installation by measuring experimentally the radial variation of shear modulus using a Spectral Analysis of Surface Waves (SASW). A 3m deep and 1m wide borehole was drilled at a site at the University of Houston, Texas in an over-consolidated (OCR > 6) stiff clay (Kalinski *et al.* 2001). The measured test results (attributed to Kalinski and Stokoe 1998) are shown in Fig. 2b. These test results indicate a radius of disturbed material, r_d, to be approximately 2 to 4 pile radii and a disturbed shear modulus value G_d of approximately half of the undisturbed value G_u. O'Neill (2001) has fitted a "probable variation" of shear modulus with radial distance through data from Kalinski and Stokoe (1998). These results are limited to the specific test and soil conditions. The authors are not aware of any high-quality test results in other deposits or for other installation methods (e.g. driven piles).

3.1 Linear radial function, *G*(*r*)

Kraft *et al.* (1981) suggested the radial variation of shear modulus could be modelled as a linear function.

$$G(r) = \begin{cases} G_u \left[(G_d/G_u) + (1 - G_d/G_u) \left(\frac{r/r_0 - 1}{r_d/r_0 - 1} \right) \right], & r \leq r_d \\ G_u \qquad\qquad\qquad\qquad\qquad\qquad , & r < r_d \end{cases} \tag{10}$$

This has been fitted through O'Neill's "probable variation" with parameters given in Fig. 2b. This equation is used to calculate G_i values at the centre of each ring. Eq. 9 is then applied to calculate the stiffness considering radially inhomogeneous soil. Fig. 3 shows the system stiffness values calculated for different G_d/G_u values (in black). The solutions from Novak and Sheta (1980) in Eq. 4 are given at $G_d/G_u = 1$. As would be expected, the systems stiffness k decreases with a reduced disturbed shear modulus G_d and an increased radius of disturbed soil r_d. This reduction in system stiffness due to the consideration of pile installation enables a more conservative calculation of the Winkler stiffness.

3.2 Power-law radial function, *G*(*r*)

Alternatively, Bateman and Crispin (2020) suggested the radial variation of shear modulus can be generalised using a power-law function:

$$G(r) = \begin{cases} G_u \left[(G_d/G_u) + (1 - G_d/G_u) \left(\frac{r/r_0 - 1}{r_d/r_0 - 1} \right)^a \right], & r \leq r_d \\ G_u \qquad\qquad\qquad\qquad\qquad\qquad , & r < r_d \end{cases} \tag{11}$$

where a is a radial inhomogeneity exponent. This equation can be simplified to Eq. 10 by setting $a = 1$. This equation has been fitted to O'Neill's "probable variation" with parameters given in Fig 2b. Eq. 9 is then applied to calculate the stiffness considering radially inhomogeneous soil (grey in Fig. 3). The power-law shear modulus variation results in a higher system stiffness than the linear due to the faster attenuation of the shear modulus towards the undisturbed value.

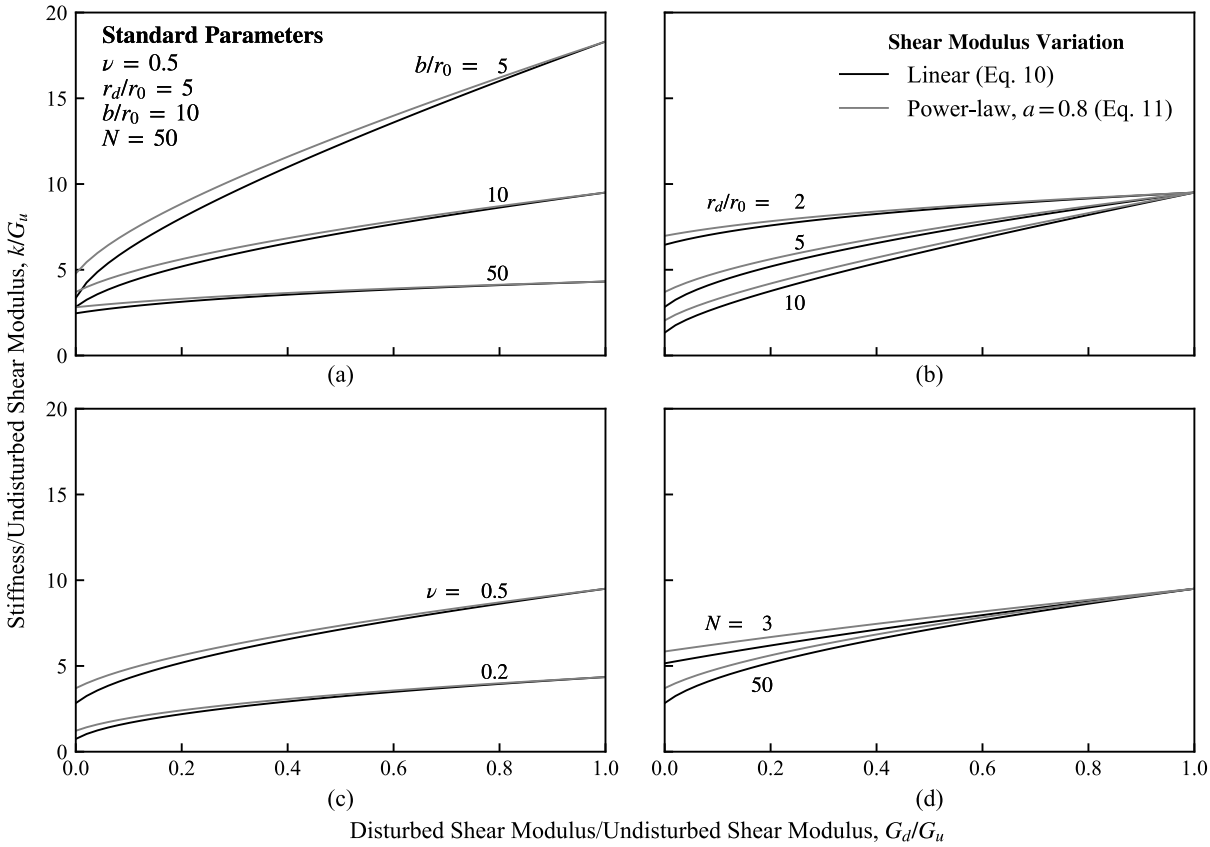

Figure 3. The stiffness of the "inner" zone of radius b (Eq. 9) with a linear (Eq. 10; black) and power-law (Eq. 11; grey) radial shear modulus variation considering the effects of (a) b/r_0, (b) r_d/r_0, (c) ν, and (d) N.

The approach derived in this paper enables any known shear modulus variation to be applied by simply allocating a single value of shear modulus G_i for each ring. This can be based on known soil conditions and the method of pile installation. A single example of a linear and power-law fit is shown above to demonstrate the suggested method. Additional numerical and experimental results are required to determine the radial inhomogeneous parameters with confidence for a specific soil-pile configuration.

4 THREE DIMENSIONAL EFFECTS

The above solution employs a two-dimensional assumption. However, evidently, the problem is three-dimensional with shear tractions τ_{rz} acting on the upper and lower surfaces of the horizontal soil slice which vary with depth (Mylonakis 2001). This adds additional complexities such as incorporation of pile stiffness, length and fixity conditions. Following Novak and Sheta (1980), superposition of the compliance of the stiffness of the "inner" annular zone k ($r_0 < r < b$; calculated above) and the "outer" annular zone k_{outer} ($b < r < \infty$) enables the overall system stiffness k_{total} to be calculated:

$$\frac{1}{k_{total}} = \frac{1}{k} + \frac{1}{k_{outer}} \tag{12}$$

Inclusion of the outer ring stiffness enables the three-dimensional effects to be incorporated. Rigorous solutions for the overall system stiffness in radially homogeneous conditions are available, usually expressed in terms of Bessel functions (Novak 1974; Crispin and Mylonakis 2022). However, these are dependent on the vertical soil profile and the pile-head fixity. Simple forms of these solutions are available by applying asymptotic forms of the Bessel functions (e.g. Mylonakis 2001; Mylonakis and Crispin 2021). Assuming, as a first approximation, the pile and "inner" region of soil act together as a fixed-head pile in vertically homogenous soil profile, k_{outer} is given by (Crispin and Mylonakis 2022):

$$k_{outer} = G_u \frac{4\,\pi\,\eta^2}{\ln(\eta) - (1+\eta^2)\,\ln\left(2\,\chi\,b\,\lambda\,\sqrt{2/3}\right)} \tag{13a}$$

$$\lambda^4 = \frac{k_{outer}}{4EI} \;,\quad EI = E_p I_p + \frac{\pi}{2}(1+\nu)\sum_{i=1}^{N} G_i\left(r_{out}^4 - r_{in}^4\right) \tag{13b}$$

where η is a compressibility coefficient (discussed by Mylonakis 2001) and taken here to be $\eta^2 = [(2-\nu)/(1-\nu)]$, $\chi = e^{\gamma}/4 \approx 0.445$ and γ is Euler's constant (≈ 0.557). λ is given in terms of EI, the sum of the flexural stiffness for the pile $E_p I_p$ and an equivalent for the "inner" soil zone. As λ in this equation is dependent on k_{outer} an iterative process would be required to solve this equation. However, Karatzia and Mylonakis (2017) suggested that only a single iteration is required with an initial value of $k_{outer} \approx 2G_u(1+\nu)$. Therefore, the overall system stiffness can be calculated by substituting both Eq. 9 for the "inner" ring and Eq. 13 for the "outer" ring into Eq. 12.

The overall stiffness (from Eq. 12) is shown in Fig. 4 for both homogeneous and radially inhomogeneous solutions. For the homogenous solution, this is compared with the more rigorous solution from Crispin and Mylonakis (2022). The "inner" annular zone is incorporated to model the soft region surrounding the pile meaning b will often be set as equal to r_d (fitted in Fig. 2b as $r_d = 3.5r_0$). At this value of b, for the homogeneous solution, incorporation of the inner zone leads to an error of around 0-8% for $\nu = 0.2$ and 45-62% for $\nu = 0.5$ (for $E_p/2G_u(1+\nu) = 100{,}1000{,}10000$). The increased error at $\nu = 0.5$ has previously been commented on by Karatzia *et al.* (2014). It is also important to note that the radially inhomogeneous solution results in a lower (more conservative) stiffness value. This indicates the importance of considering the effect of pile installation.

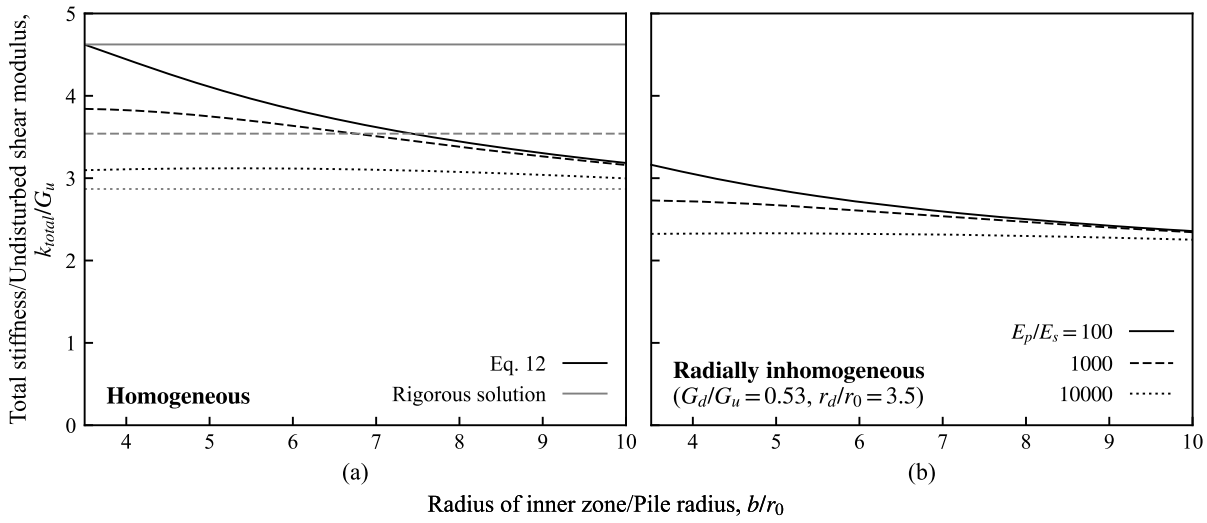

Figure 4. The overall stiffness of the system (Eq. 12) for a fixed head pile in (a) radially homogenous (compared with the more rigorous 3D solution detailed in Crispin and Mylonakis 2022), (b) radially inhomogeneous conditions. ($N = 500$, $\nu = 0.2$)

5 CONCLUSIONS

A simplified method to develop "*p-y*" curves considers a horizontal slice of soil with an "inner" and "outer" annular zone of soil (Fig. 1). The "inner" zone can be used to consider pile installation effects, which may result in reduced soil stiffness close to the pile circumference. To this end, this paper:

- Derives an improved solution for the system stiffness of the "inner" zone by considering the effects of pile installation (Eq. 9).
- Provides an example of calculating stiffness of the "inner" zone by considering two variations of shear modulus with radial distance: a linear (Eq. 10) and a power-law (Eq. 11) function. These are fitted through experimental data from Kalinski and Stokoe (1998).

- Discusses the calculation of the overall system stiffness through the inclusion of the "inner" and "outer" zones (Eq. 12).

ACKNOWLEDGEMENTS

Thanks are due to Dr. Jamie Crispin for his helpful discussions about the three-dimensional effects. The first author would like to thank EPSRC for their support (grant number EP/T517872/1).

REFERENCES

Baguelin, F., Frank, R., and Saïd, Y.H. (1977). Theoretical study of lateral reaction mechanism of piles. *Géotechnique*, 27(3), 405-434. https://doi.org/10.1680/geot.1977.27.3.405.

Bateman, A. H., and Crispin, J. J. (2020). Theoretical "*t-z*" curves for piles in radially inhomogeneous soil'. *DFI Journal: The Journal of the Deep Foundations Institute*, 14(1): 1–9. https://doi.org/10/gmdjpc.

Bateman, A. H., Mylonakis, G., and Crispin, J. J. (2023). Simplified analytical 'm-θ' curves for predicting nonlinear lateral pile response. Under Review.

Byrne, B. W., Houlsby, G. T., Burd, H. J., Gavin, K. G., Igoe, D. J. P., Jardine, R. J., Martin, C. M., McAdam, R. A., Potts, D. M., Taborda, D. M. G., and Zdravković, L. (2020). PISA design model for monopiles for offshore wind turbines: application to a stiff glacial clay till. *Géotechnique*, 70(11), 1030–1047. https://doi.org/10.1680/jgeot.18.P.255.

Crispin, J. J., and Mylonakis, G. (2022). Exact Winkler solution for laterally loaded piles in inhomogeneous soil. *Journal of Engineering Mechanics*, ASCE, 148(11), 04022065. https://doi.org/jjhj.

El Naggar, M. H. (2000). Vertical and torsional soil reactions for radially inhomogeneous soil layer. *Structural Engineering and Mechanics*, 10(4), 299–312. https://doi.org/jjhp.

Han, Y., and Sabin, G. (1995). Impedances for radially inhomogeneous viscoelastic soil media. *Journal of Engineering Mechanics*, ASCE, 121(9), 939–947. https://doi.org/fmtst3.

Kalinski, M. E., and Stokoe, K. H. (1998). *Stress wave measurements in open holes in soil*. Final Report, Department of Civil Engineering, University of Texas at Austin, Texas, US.

Kalinski, M. E., Ata, A., Stokoe, K. H., and O'Neill M. W. (2001). Use of SASW measurements to evaluate the effect of lime slurry conditioning in drilled shafts. *Journal of Environmental and Engineering Geophysics*, 6(4): 147–56. https://doi.org/10.4133/jeeg6.4.147.

Karatzia, X., and Mylonakis, G. (2017). Horizontal stiffness and damping of piles in inhomogeneous soil. *Journal of Geotechnical and Geoenvironmental Engineering*, ASCE, 143(4), 04016113. https://doi.org/gmvf4r.

Karatzia, X., Papastylianou, P., and Mylonakis, G. (2014). Horizontal soil reaction of a cylindrical pile segment with a soft zone. *Journal of Engineering Mechanics, ASCE*, 140(10): 04014077. https://doi.org/f6hsjw.

Kraft, L. M., Ray, R. P. and Kagawa, T. (1981) Theoretical t-z Curves. *Journal of the Geotechnical Engineering Division, ASCE*, 107(11): 1543–61. https://doi.org/10.1061/ajgeb6.0001207.

Lakshmanan, N., and Minai, R. (1981). Dynamic soil reactions in radially non-homogeneous soil media. *Bulletin of the Disaster Prevention Research Institute*, 31(2), 79–114.

Michaelides, O., Gazetas, G., Bouckovalas, G., and Chrysikou, E. (1998). Approximate non-linear dynamic axial response of piles. *Géotechnique*, 48(1), 33–53. https://doi.org/d2g7zz.

Mylonakis, G. (2001). Elastodynamic model for large-diameter end-bearing shafts. *Soils and Foundations*, 41(3), 31–44. https://doi.org/d9j85t.

Mylonakis, G., and Crispin, J. J. (2021). *Simplified models for lateral static and dynamic analysis of pile foundations*. In A. M. Kaynia (Ed.), Analysis of Pile Foundations Subject to Static and Dynamic Loading (1st ed., pp. 185–245). CRC Press. https://doi.org/h7t2.

Novak, M., Aboul-Ella, F., and Nogami, T. (1978). Dynamic soil reactions for plane strain case. *Journal of the Engineering Mechanics Division*, ASCE, 104(4), 953–959. https://doi.org/gmdjsj.

Novak, M. and Sheta, M. (1980). Approximate approach to contact effects of piles. In M.W. O'Neill and R. Dobry, *Dynamic response of pile foundations, analytical aspects: Proceedings of a session*. ASCE. 53-79.

O'Neill, M. W. (2001). Side resistance in piles and drilled shafts. *Journal of Geotechnical and Geoenvironmental Engineering, ASCE*, 127(1): 3–16. https://doi.org/10.1061/(asce)1090-0241(2001)127:1(3).

Veletsos, A. S., and Dotson, K. W. (1988). Horizontal impedances for radially inhomogeneous viscoelastic soil layers. *Earthquake Engineering & Structural Dynamics*, 16(7), 947–966. https://doi.org/dbbrcj.